



Record 2021/04 | eCat 134038

Exploring for the Future—Remodelling the Oolloo–Jinduckin interface across the Daly Basin, Northern Territory

Interpreting stratigraphic boundaries using probabilistic airborne electromagnetic inversions

N.J. Symington, A.M. Haiblen, A. Ray, S.J. Tickell and L.J. Gow

Exploring for the Future—Remodelling the Oolloo–Jinduckin interface across the Daly Basin, Northern Territory

Interpreting stratigraphic boundaries using probabilistic airborne electromagnetic inversions

GEOSCIENCE AUSTRALIA
RECORD 2021/04

N.J. Symington¹, A.M. Haiblen¹, A. Ray¹, S.J. Tickell² and L.J. Gow¹

1. Geoscience Australia
2. Northern Territory Department of Environment and Natural Resources (DENR)

Department of Industry, Science, Energy and Resources

Minister for Resources, Water and Northern Australia: The Hon Keith Pitt MP
Secretary: Mr David Fredericks PSM

Geoscience Australia

Chief Executive Officer: Dr James Johnson

This paper is published with the permission of the CEO, Geoscience Australia

Geoscience Australia acknowledges the traditional custodians of the country where this work was undertaken. We also acknowledge the support provided by individuals and communities to access the country, especially in remote and rural Australia.



© Commonwealth of Australia (Geoscience Australia) 2021

With the exception of the Commonwealth Coat of Arms and where otherwise noted, this product is provided under a Creative Commons Attribution 4.0 International Licence.

(<http://creativecommons.org/licenses/by/4.0/legalcode>)

Geoscience Australia has tried to make the information in this product as accurate as possible. However, it does not guarantee that the information is totally accurate or complete. Therefore, you should not solely rely on this information when making a commercial decision.

Geoscience Australia is committed to providing web accessible content wherever possible. If you are having difficulties with accessing this document please email clientservices@gov.au.

ISSN 2201-702X (PDF)

ISBN 978-1-922446-34-3 (PDF)

eCat 134038

Bibliographic reference:

Symington, N.J., Haiblen, A.M., Ray, A., Tickell, S.J. & Gow, L.J. 2021 *Exploring for the Future — Remodelling the Oolloo–Jinduckin interface across the Daly Basin: Interpreting stratigraphic boundaries using probabilistic airborne electromagnetic inversions*, NT. Record 2021/04, Geoscience Australia, Canberra <http://dx.doi.org/10.11636/Record.2021.004>

Executive summary

This report presents key results from the Daly River groundwater project conducted as part of Exploring for the Future (EFTF)—an Australian Government funded geoscience data and information acquisition program. The four-year (2016–20) program focused on better understanding the potential mineral, energy and groundwater resources in northern Australia.

In this investigation we use models of sub-surface bulk electrical conductivity within the geological Daly Basin to model the depth of the interface between the Jinduckin Formation and the overlying Oolloo Dolostone. The Oolloo Dolostone is the most productive aquifer in the Daly Basin, while the Jinduckin Formation is an aquitard separating the Oolloo from the deeper Tindall Limestone aquifer. Airborne electromagnetic (AEM) data acquired across the basin were inverted with both deterministic and stochastic methods to generate a suite of bulk electrical conductivity models. Comparison with boreholes suggests that the Jinduckin Formation is significantly more conductive than the Oolloo Dolostone and the interface between them is well resolved in these AEM conductivity models. We developed an interactive plot for visualising the probability distribution of bulk conductivities for AEM points inverted with the stochastic inversion routine. We interpreted 389 AEM points using this approach and used interpolation to derive a new stratigraphic Oolloo–Jinduckin surface. The new surface is generally deeper than current models of the interface, which were derived by interpolating stratigraphic picks from boreholes. In the data-sparse southwest of the Daly Basin the new geological surface interpreted from the AEM is significantly deeper than the previous model. New drilling, geophysics and other field data from data-sparse areas of the basin are required to validate and refine our model. This new interface can be used to better constrain aquifer architecture in groundwater flow modelling and support groundwater management of this region. The method developed for interpreting stratigraphy directly from the posterior probability distribution of electrical conductivity is applicable for other geophysical interpretation tasks.

Contents

1 Introduction	1
1.1 Physiography	1
1.2 Geology	2
1.3 Geological models	3
1.4 Hydrogeology	4
2 Airborne Electromagnetic Methods	5
2.1 Acquisition	5
2.2 Geophysical inversion	6
2.3 Stratigraphic interpretation from AEM inversion models	7
2.4 Workflow for interpreting stratigraphy from AEM inversion models	8
3 Results	12
3.1 Borehole comparison	12
3.2 Modelling Stratigraphy	14
3.3 Comparison with existing Oolloo–Jinduckin surface in DENR2018 model	16
4 Discussion	17
4.1 Methodology appraisal and new interpretation	17
4.2 Hydrogeological implications	18
5 Conclusions	20
6 Recommendations	21
7 Acknowledgements	22
8 References	23

List of Figures

Figure 1.1. Geology of Daly Geological Basin.....	2
Figure 2.1. Map of geophysical data acquisition	6
Figure 2.2. The pmap for an airborne electromagnetics (AEM) sounding near borehole RN006825	9
Figure 2.3. The pmap for an AEM sounding with no borehole control.....	11
Figure 3.1 Vertically gridded conductivity section of flight line #103601	12
Figure 3.2 The pmap for the nearest airborne electromagnetic (AEM) sounding to borehole RN032097	13
Figure 3.3. Maps interpreted Ooloo–Jinduckin interface as interpreted using AEM in this study (A) and using borehole and geological data in a previous study (B).....	15
Figure 3.4 Vertically gridded conductivity section of flight line #109201.....	16

List of Tables

Table 3.1 Comparison between the elevation (m AHD) of the Ooloo–Jinduckin interface interpreted from borehole data and the nearest AEM sounding.....	13
--	----

List of Abbreviations

ABBREVIATION	
AEM	Airborne Electromagnetics
EFTF	Exploring for the Future
DENR	Northern Territory - Department of Environment and Natural Resources
BOM	Bureau of Meteorology
GA	Geoscience Australia
GARJMCMTDEM	Reversible-Jump Markov Chain Monte Carlo
MGBL	Metres Below Ground Level
MAHD	Metres Above Australia Height Datum

1 Introduction

The Australian Government's Exploring for the Future (EFTF) Program received \$100.5 million for four-years in 2016. The Program's objective over the four years from 2016-2020 was to provide a holistic picture of the potential mineral, energy and groundwater resources in northern Australia. The program has delivered new geoscience data, knowledge and decision tools to support increased industry investment and sustainable economic development across the north. Further detail is available at (<http://www.ga.gov.au/eftf>).

Groundwater is a critical resource that accounts for most water used across northern Australia. The groundwater component of the EFTF program focused on addressing groundwater resource knowledge gaps to support future opportunities for economic development via irrigated agriculture, extractive industries and increased security of community water supplies. Through collaboration with state and territory partners, the program undertook targeted regional investigations of groundwater systems and assessments of groundwater potential more broadly across the region.

The program's activities, implemented by Geoscience Australia, involved application of innovative geoscience tools to collect, integrate and analyse a range of data. The activities included geological and hydrogeological data; airborne and ground-based geophysical and hydrogeochemical surveys; remote sensing data; and stratigraphic drilling. The new data and better understanding of groundwater systems also helps inform decision-making about groundwater use to protect environmental and cultural assets. These outcomes strengthen investor confidence in resources and agricultural projects by de-risking groundwater in northern Australia.

AEM is a geophysical technique that enables rapid estimation of sub-surface electrical conductivity across vast swathes of land. It is thus well suited to investigating many Australian groundwater systems, where there is typically a paucity of high-quality geoscientific data. In this investigation we used AEM to reinterpret the interface between the Jinduckin Formation and overlying Ooloo Dolostone. This mapped product will enable future groundwater flow models to represent the geometry of the Ooloo Dolostone more accurately. Groundwater hydrochemistry and borehole induction and gamma data were also acquired as part of this study. While the results are not reported here, the data are available through the EFTF portal (<https://portal.ga.gov.au/>).

1.1 Physiography

The Daly geological basin underlies much of the central part of the Daly River surface water catchment, around 200 km south of Darwin in the Northern Territory. The region is particularly dependent on groundwater for town supply, irrigated agriculture, tourism, ecosystems, springs and Indigenous culture. With combined environmental, economic and cultural demands on the groundwater resource, water management and planning decisions require high-quality geoscientific data to better characterise the sub-surface. The Daly Basin is in the wet-dry tropics of northern Australia. More than 95% of the mean annual rainfall occurs between November and April, resulting in highly seasonal streamflow and groundwater recharge. Rainfall is up to 30% higher in the north of the catchment (CSIRO, 2009).

The Daly River and its tributaries are some of the only perennial rivers in the Northern Territory, with dry season streamflow dependent on groundwater baseflow. The river supports important aquatic and

riparian ecosystems and is culturally significant to Indigenous people and the wider community. As the groundwater and surface water are highly connected, management decisions are based on an integrated understanding of the surface water – groundwater system (Knapton, 2011).

1.2 Geology

The Daly geological basin is composed of Cambrian to Ordovician (~541-470 Ma) carbonate and siliciclastic rocks, unconformably overlain by Cretaceous rock of the onshore Carpentaria Basin (Kruse & Munson, 2013) (Figure 1.1). The basin is a northwest elongated synform about 170 km long and 30 km wide. The formations dip basin-wards at shallow angles, generally less than 1°. The basin formed through prolonged sedimentary deposition in the shallow seas of the Centralian Superbasin with mild syn-sedimentary sagging, probably along basin-scale faults (Kruse & Munson, 2013).

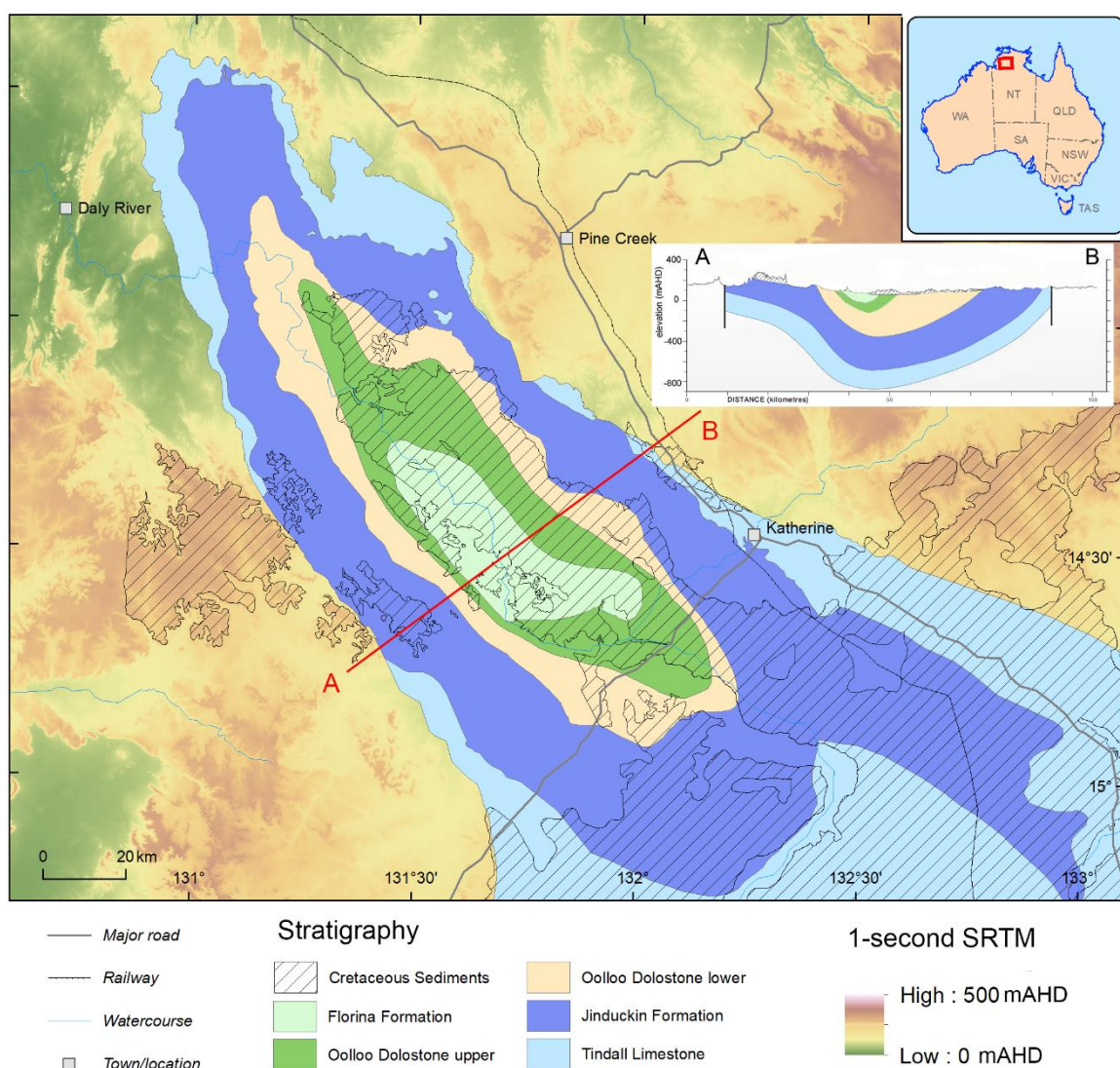


Figure 1.1. The extents of the Cambrian to Cretaceous sedimentary units from the Daly geological basin. Inset is a cross-section of stratigraphy through the basin.

The Cambrian Daly River Group is the most hydrogeologically significant group in the basin, with a maximum recorded thickness of 709 m in the stratotype section in cored drill hole NTGS86/1 (Kruse et al., 1990). The group has three constituent units: the Tindall Limestone, Jinduckin Formation and Oolloo Dolostone. For a detailed description of these stratigraphic units refer to Kruse and Munson (2013).

The basal Tindall Limestone consists of grey, mottled limestone, with minor intercalated maroon-green siltstone or dark grey mudstone. The boundary between the Tindall Limestone and overlying Jinduckin Formation is conformable and characterised by an abrupt upward change from limestone to more siliciclastic rock. This transition represents a change from deposition in an open-shelf marine to a dominantly peri-tidal environment (Kruse & Munson, 2013).

The Jinduckin Formation consists of maroon-green dolomitic-siliciclastic siltstone with dolomitic sandstone–siltstone interbeds, local lenses of dolostone and dolomitic quartz sandstone. The siltstone-dominated Jinduckin Formation passes upwards into the carbonate-dominated Oolloo Dolostone with a conformable and transitional contact. The interface between the Jinduckin Formation and Oolloo Dolostone was defined in water bores by correlating gamma logs and interpreting driller's logs (Tickell, 2011). The top of the Jinduckin Formation was picked at the 'highest finely laminated dolomitic sandstone–siltstone interbeds' in the sequence. Although the transitional nature of the contact makes the definition of an interface from such scarce data difficult, there does appear to be an appreciable change in electrical conductivity as we discuss in Section 3.1.

The Oolloo Dolostone comprises two members: the well-bedded lower Briggs Member and the massive upper King Member. The Briggs Member comprises fine- to medium-grained, crystalline dolostone, dolograinstone, doloboundstone and dolomitic quartz sandstone. The Daly River Group is capped by the Ordovician Florina Formation and comprises a succession of three carbonate intervals separated by two fine-grained, glauconite-bearing quartz sandstone units (Tickell et al., 2015). The Florina Formation and the Daly River Group are unconformably blanketed by the Carpentaria basin's Cretaceous claystone and sandstone over a substantial portion of the Daly Basin (Figure 1.1).

1.3 Geological models

Three-dimensional (3D) models of the Oolloo–Jinduckin interface have been developed by the Bureau of Meteorology (BOM) and Northern Territory Department of Environment and Natural Resources (DENR). Both modelling endeavours interpreted the surface by interpolating stratigraphic data from the DENR registered bore database and hand-drawn stratigraphic horizon contours based on these boreholes (Tickell et al., 2015). The BOM generated a web-based 3D visualisation of the Tindall Limestone aquifer, the Jinduckin Formation aquitard, the Oolloo Dolostone aquifer, the Florina Formation aquifer and the Cretaceous sediments (BOM, 2017). A 3D model of the major formation boundaries was created for DENR using the 3D geological modelling package *Leapfrog*. This model will be referred to as the 'DENR2018' model henceforth, and will be the existing model that we discuss in the rest of this report. The borehole data used to derive surfaces for both models are sparse, unevenly distributed and of variable quality (Figure 2.1). As previously mentioned, a lack of unambiguous marker horizon demarcating the change from aquifer to aquitard was another major issue in 3D modelling.

1.4 Hydrogeology

There are two major fractured and karstic aquifers in the Daly Basin; the Tindall Limestone and Ooloo Dolostone aquifers, hosted by their respective geological formations. These aquifers are widespread sheet-like features best developed in the weathered zone, with interconnected cavities and fractures in the host rock formed by carbonate dissolution due to groundwater movement. High-yielding (>50 L/s) bores intersect submerged cavities, voids and fractures in the rock which are commonly visible at the surface in the form of sinkholes where a cavity has collapsed (CSIRO, 2009; Tickell, 2011). While it acts predominantly as an aquitard, the Jinduckin Formation contains thin local aquifers within limestone beds in some areas. Both aquifers are in connection with small-scale sandstone aquifers from the overlying Cretaceous sediments.

Recharge to the groundwater system occurs in the wet season when there is sufficient rainfall. Recharge over uncleared land is dominated by bypass flow (70%), where the water seeps through macropores and/or dissolution features and has minimal interaction with the unsaturated zone (CSIRO, 2009). Recharge is highly spatially variable due to the strong north–south rainfall gradient across the basin and the presence of the Cretaceous clay, which acts to limit recharge for most of its extent.

Within the Ooloo Dolostone, groundwater flows from the southeast towards the thickest parts of the basin, where it mostly discharges into the Daly River (Tickell, 2009). Flow in the Tindall Limestone is more complex, with at least six separate groundwater catchments. Groundwater generally flows along the margins of the basin where the limestone aquifer is unconfined, with only minor flow in the confined part of the basin (Tickell, 2009).

Both the Tindall and Ooloo aquifers contribute more than 10 m³/s of baseflow to the Daly River (Knapton et al., 2010). Groundwater discharge occurs in reaches where the river has incised the aquifers either through a diffuse riverbed regime or discrete spring. Groundwater is extracted from both aquifers, mainly for irrigation but also for stock and domestic purposes. A much smaller amount of water is taken directly from the rivers. While a discussion of water management is outside of the scope of this report, we note that it is informed by both groundwater flow modelling (Knapton, 2005, 2006) and coupled groundwater – surface water flow modelling (Knapton, 2011).

2 Airborne electromagnetic methods

AEM is a geophysical technique that enables rapid estimation of sub-surface electrical conductivity across vast swathes of land. AEM involves transmitting an electromagnetic signal from a system attached to a helicopter or plane and measuring the response from eddy currents induced in the sub-surface. Bulk electrical conductivity is sensitive to sub-surface properties, including groundwater salinity, mineralogy, porosity and lithology. As a consequence, AEM is increasingly being used in groundwater investigations for a variety of applications (Siemon et al., 2009) including mapping stratigraphy (Korus et al., 2017; Roach & McPherson, 2016) and estimating groundwater salinity (Kirkegaard et al., 2011; Symington et al., 2020; Viezzoli et al., 1997). AEM data were acquired across the Daly Basin to allow for reconnaissance scale mapping and modelling of stratigraphic units. The AEM data were then processed to provide a foundation to interpret basin stratigraphy.

2.1 Data acquisition

AEM data were acquired with the SkyTEM™ 312-FAST® system in July and August 2017. In total 3512 line km of AEM data were acquired along lines spaced at 1000 m, 2000 m or larger intervals (up to 30 000 m; Figure 2.1). The lines predominantly run with an east–west or north-easterly orientation to cross the long axis of the basin and important structures at high angles. A smaller number of lines were flown along the long axis of the basin. We refer the reader to the Data Acquisition and Processing Report (Ray et al., 2020b) for more technical detail on the survey.

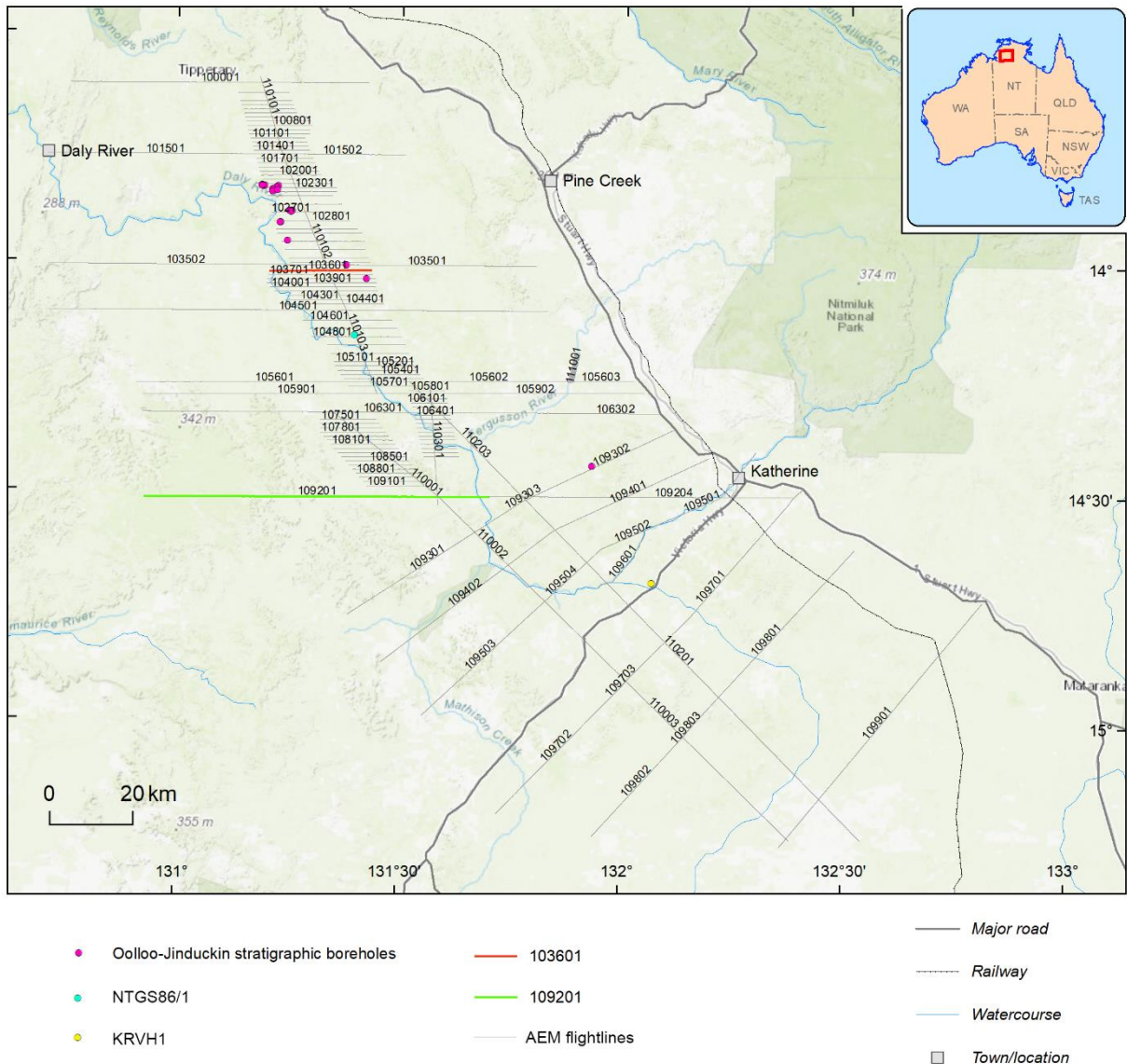


Figure 2.1 A map showing the airborne electromagnetic (AEM) flight lines and borehole data acquired as part of the Daly River project. The highlighted lines are plotted as sections in Figure 3.1 and Figure 3.4. The Oolloo–Jinduckin stratigraphic bores on this map are described in Table 3.1. Boreholes NTGS86/1 and KRVH1 are the boreholes with cored intervals across the Oolloo–Jinduckin interface.

2.2 Geophysical inversion

Raw AEM data itself is not interpretable in a physically meaningful way. However, the data can be used to infer the bulk electrical conductivity of the sub-surface. For a given bulk conductivity model of the sub-surface and set of data acquisition parameters, we can use the electromagnetic governing equations to estimate the likely data response, which is the data we would expect to acquire using AEM. This process, where models are used as inputs to produce the data response, is known as forward modelling. Inversion is the inverse of the forward modelling—it is a mathematical technique for recovering the model from the observed geophysical measurements. For this study, the data were modelled using deterministic and stochastic inversion methods, which we describe below.

Deterministic geophysical inversions use optimisation routines to determine the bulk conductivity model that ‘best’ fits the AEM data given specified noise levels. This is done by trying many models and iteratively approaching the best model by reducing the misfit between our forward model response and our data. For this study we used the Aarhus Workbench LCI inversions (Auken et al., 2005) that were provided by SkyTEM™ as part of the AEM data package (Ray et al., 2020b). This algorithm inverts every AEM sounding simultaneously using the assumption of one-dimensional (1D) geology, where each AEM layer is laterally continuous. The algorithm then applies both horizontal and vertical smoothness constraints. While these inversions are quick to run and relatively straightforward to visualise, they suffer from model non-uniqueness, where many models will adequately fit the same data to within noise (Tarantola, 2006). Furthermore, the non-linear nature of AEM inversion makes estimations of model uncertainty difficult (refer to Ray et al. (2020a) for broader discussion of issues with deterministic inversions).

To address deterministic model uncertainty, selected AEM soundings were also inverted using the Geoscience Australia reversible-jump Markov chain Monte Carlo (GARJCMCDEM) stochastic inversion algorithm (Brodie & Richardson, 2015). In contrast to the deterministic inversions, this routine inverts the data tens of thousands of times to produce an ‘ensemble’ of models, which adequately fit the AEM data given the noise levels. The advantage of this approach is that we can estimate the posterior probability distribution of the model parameters using the model ensemble. These distributions of sub-surface electrical conductivity enable the interpreter to understand model uncertainty and the confidence with which they can interpret the conductivity models.

2.3 Stratigraphic interpretation from AEM inversion models

Bulk electrical conductivity in the sub-surface is a function of variables such as the composition of rock or sediment, groundwater salinity, aquifer porosity and saturation, cementation and tortuosity. While estimation of bulk conductivity models from AEM data is relatively straightforward using geophysical inversion, mapping stratigraphy from these models is difficult and time-consuming and relies on the judgment and skill of the interpreter. Picking an interface between two stratigraphic units from a conductivity model (or an ensemble of models) is possible only if the units have sufficient conductivity contrast to be resolved from the AEM data. This is relatively simple when imaging highly conductive bodies such as a massive sulphide deposit within resistive host rocks. However, in many cases, the combination of sub-surface parameters that influence bulk conductivity yield a very complex response. Therefore, interpretations made using a single ‘best fit’ AEM inversion, which is but one of many models that fit the observed data, are commonly problematic. Therefore, multiple AEM inversion models are preferred, coupled with an uncertainty analysis, to underpin confidence in data and provide a robust interpretation.

In this study we interpreted ensembles of AEM bulk conductivity models to estimate the depth and extent of the stratigraphic interface between the Ooloo Dolostone and the Jinduckin Formation. We first observed AEM models proximal to boreholes where the Ooloo–Jinduckin interface has been interpreted primarily from gamma log data. The purpose of this was to assess how consistent the borehole stratigraphic picks were with the AEM models and to ascertain if the two units had sufficiently different bulk conductivities to allow interpretation away from boreholes. The results of this initial assessment allowed us to apply an appropriate interpretation strategy.

To better understand uncertainty relating to model non-uniqueness, we interpret not only the LCI inversions but also the GARJCMCDEM stochastic inversions (see Section 2.2). Following the sounding-based interpretation, we converted the interpreted surface from metres below ground level (m BGL) to elevation relative to the Australian Height Datum (m AHD). We used the Topo to Raster

algorithm (Hutchinson, 1989) to create a gridded surface from point elevations and clipped the raster to our best estimate of the extent of the interface.

2.4 Workflow for interpreting stratigraphy from AEM inversion models

In this study we interpreted the depth of boundary of the Jinduckin Formation and Oolloo Dolostone using conductivity models produced by the deterministic LCI AEM inversion and the ensemble of stochastic GARJCMCDEM inversions. From the GARJCMCDEM model ensemble we can find the probability distribution, or posterior distribution, for the bulk conductivity for each depth interval. Having access to the posterior distribution of AEM model parameters gives the interpreter the ability to make interpretations that are more appropriate given model parameter uncertainty. However, visualising the distributions is a significant challenge. Below, we explain the AEM inversion visualisation approach that the AEM interpreter used during this study and provide some examples.

In Figure 2.2 we present the probability map plots that were used for the interpretation of the AEM inversions. These plots help visualise the LCI and GARJCMCDEM inversion data for a single sounding, as well as providing useful contextual information to aid the interpreter. The figure caption provides a detailed explanation of what is visualised in the various panels. These plots were produced in a Jupyter notebook environment (Kluyver et al., 2016) allowing the interpreter to customise the plots by changing for example the colour scale, depth and spatial resolution of the plots. These plots are interactive and allow the interpreter to click on the probability plot to add their interpretation of the Oolloo–Jinduckin interface depth from the inversion. This interpretation gets saved into memory and written to disk for later processing within the Geographic Information System (GIS).

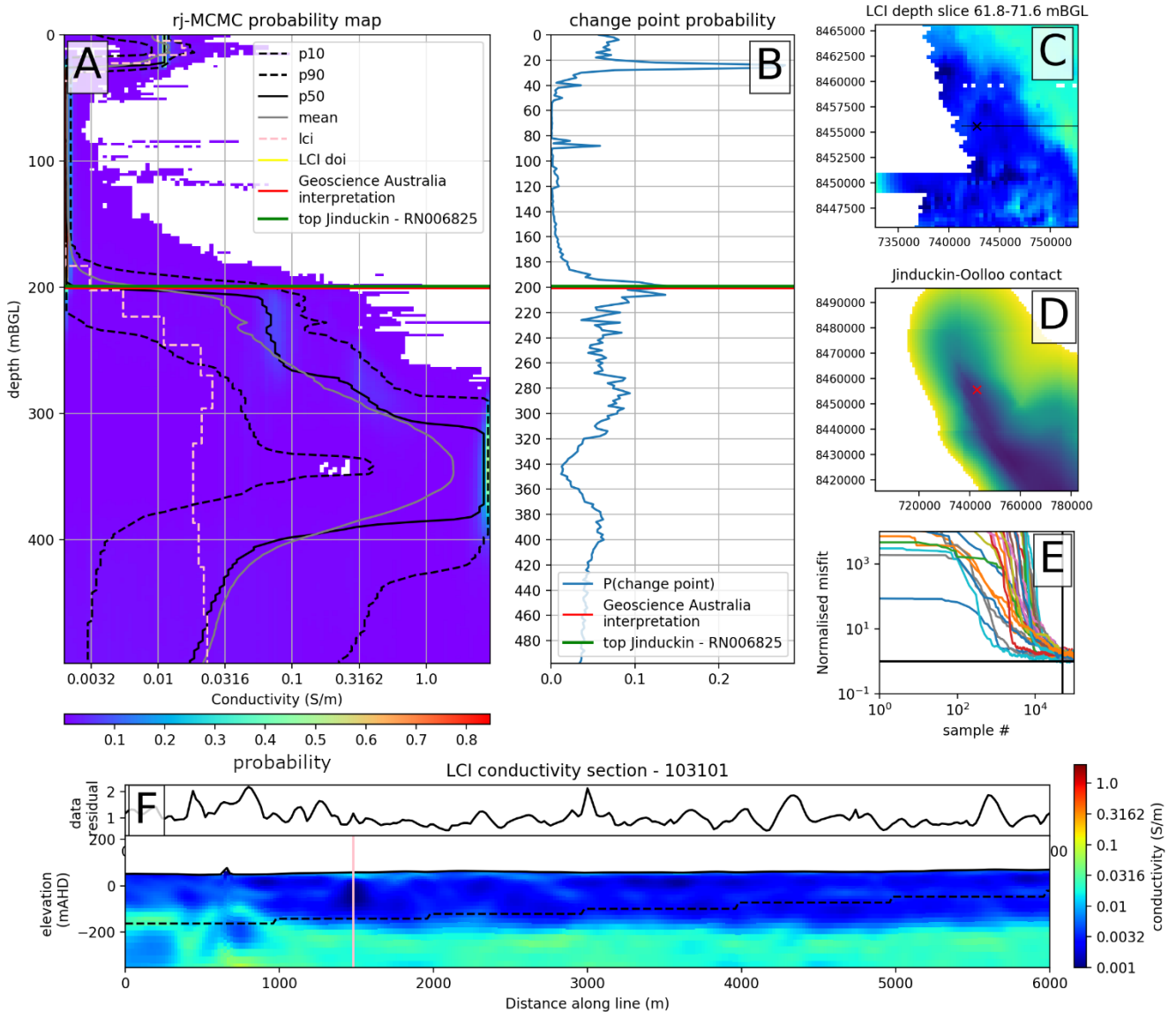


Figure 2.2. The probability map plots used for interpreting airborne electromagnetics (AEM) data: (A) probability of conductivity with depth, also known as a probability map. Warmer colours represent high probability of conductivity at a particular depth, while cooler colours are less probable. White areas indicate near-zero probability. On the pmap are the mean, 10th (p10), 50th (p50) and 90th (p90) percentile conductivities from the GARJMCCTDEM. The LCI profile is shown with a dashed line. We also plot the DENR2018 depth to Oolloo–Jinduckin interface as a guide; (B) the probability of an AEM conductivity interface occurring at a particular depth; (C) conductivities in the 61.8 to 71.6 m below ground level (mBGL) LCI depth slice with the AEM flight line and sounding location plotted on top; (D) The Bureau of Meteorology (BOM) Oolloo–Jinduckin interface surface (m AHD) with the AEM sounding location plotted with a red 'x'; (E) a plot of convergence for each of the 16 probabilistic inversion runs at this sounding. A normalised misfit of ~1 is the criterion for convergence; (f) a vertical LCI conductivity section with the associated misfit. The BOM Oolloo–Jinduckin interface is the black dashed line plotted on top.

Our approach for interpreting the Oolloo–Jinduckin interface at a single sounding using plots like Figure 2.2 and Figure 2.3 was:

- Assess GARJMCCTDEM and LCI model convergence using panels (e) and (f) respectively.
- If model(s) have converged to approximate 1.0, observe the AEM conductivity distribution results in panel (A).

- If there are stratigraphic boreholes within 500m of the sounding plot them on panel (a) and panel (b). Determine how the stratigraphic borehole interpretation or the DENR2018 interface compares with the LCI conductivity and GARJMC MCMC conductivity probabilities. If there are significant difference, attempt to reconcile this using the original borehole data or by considering the likely resolution of each method. This is discussed further in Section 3.1.
- If we identify a significant increase in conductivity in both the p10 and p90 models, as we do at around 200 m depth (Figure 2.2b), we may pick this depth using the most probable AEM layer depth in the vicinity using panel (B). This implies that the middle 80% of all models show an increase in conductivity and thus we are ‘reasonably’ confident that this increase is supported by the data. The peak of the change point probability histogram represents the local maximum likelihood of a conductivity boundary according to the model ensemble and is thus the most appropriate choice for an interpreted boundary.
- If the increase in conductivity is below what we can interpret with ‘reasonable’ confidence, we may pick it if we believe it still represents a better estimate of the depth to interface than the DENR2018 model. This may occur if the probability map suggests that the current estimate is inconsistent with the AEM conductivities and inferred geological structure in the area (for example, Figure 2.3).
- If we cannot identify an appreciable increase in bulk conductivity then we do not interpret the point.

From the method described above, it is clear that the interpreter is still required to use their scientific judgment based on their experience and context. The workflow and visualisation tool is designed to allow a skilled interpreter of AEM data to have easy access to a visualisation, such that they can rapidly utilise AEM conductivity models to support their interpretation. Our workflow is similar to that described by Blatter et al. (2018) for using trans-dimensional inversions of AEM data to interpret briny water beneath a glacier. However, their methodology was not interactive and was performed for a much smaller number of soundings due to computational constraints overcome by the GARJMC MCTDEM algorithm.

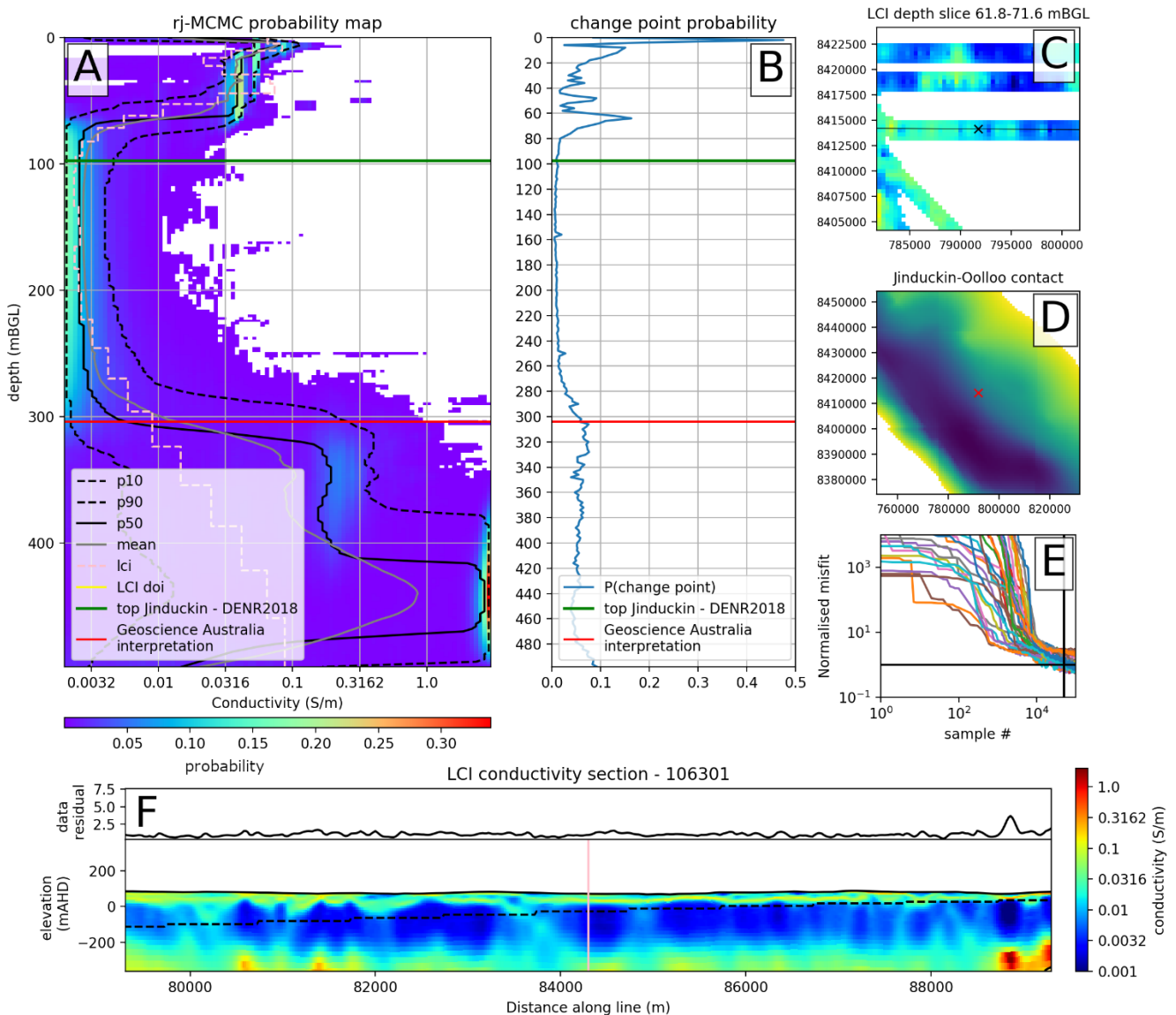


Figure 2.3 Plots for a sounding with poorly resolved Oolloo–Jinduckin interface. Panels as described in Figure 2.2. Note that the DENR2018 model shows the top of the Jinduckin Formation at about 70 m depth, which is inconsistent with observations in the area that the Jinduckin Formation is far more conductive. Despite there being no significant peak in the change point probability histogram (panel b) at depth, our interpretation of an interface at 275 mBGL is a significant improvement on the virtually unconstrained 70m depth from the DENR2018 model.

3 Results

In this section we describe the outcome of interpreting the Oolloo–Jinduckin interface from AEM conductivity models. We first describe the comparison between AEM picks and nearby stratigraphic boreholes. We then describe the results of interpreting the interface across the entire basin based on the newly interpreted picks. Finally, we compare the surface generated as part of this study with the DENR2018 surface.

3.1 Borehole comparison

Fifteen stratigraphic boreholes from the DENR boreholes database fulfilled the criteria of having intersected the Oolloo Dolostone – Jinduckin Formation interface and being located within 500 m of an AEM sounding. As touched on in Section 2.4, our initial visualisation of the AEM conductivity models indicated that there was generally a transition from a resistor to a deeper, moderate conductor around the Oolloo–Jinduckin interface from the DENR2018 model (e.g. Figure 3.1). Based on our understanding of the lithology of the two units and our observation of bulk conductivity profiles at the 15 boreholes, we assumed that this conductivity boundary represents a significant change in lithology and was a mappable interface between the two units.

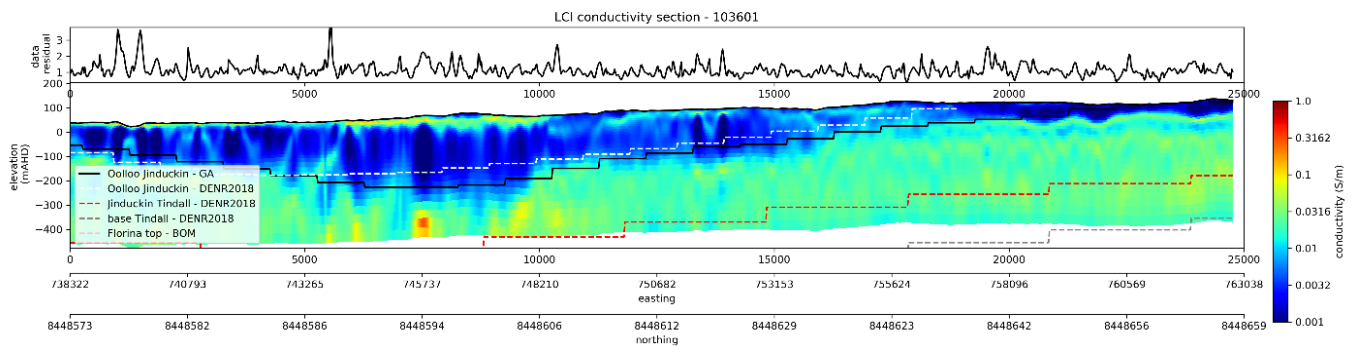


Figure 3.1 Vertically gridded LCI conductivity section of flight line #103601 and associated data misfit from the north of the Daly River Basin. This section demonstrates the well-resolved and laterally consistent conductivity contrast that characterises the transition from the Jinduckin Formation to the overlying Oolloo Dolostone.

The results from interpreting the Oolloo–Jinduckin interface from the AEM soundings near stratigraphic boreholes are shown in Table 3.1. At some boreholes (e.g. RN006825, Figure 2.2; RN032097, Figure 3.2) the two datasets provide similar results, whereas in other areas there are significant differences (e.g. RN031100). The root mean squared difference in interpreted Oolloo–Jinduckin elevation between the AEM-derived estimates and borehole data is 28.5 m, the standard deviation is 25.0 m and the mean difference about 15.1 m, where a positive value indicates that the AEM-derived estimates are more likely to interpret the interface deeper than the borehole-derived estimates. There are significant uncertainties associated with the borehole interpretations, as we will explain in Section 4.1. While a fifteen stratigraphic boreholes and proximally located AEM soundings is not a large enough sample size for a statistically significant comparison, it is still a useful exercise for qualitatively assessing both datasets.

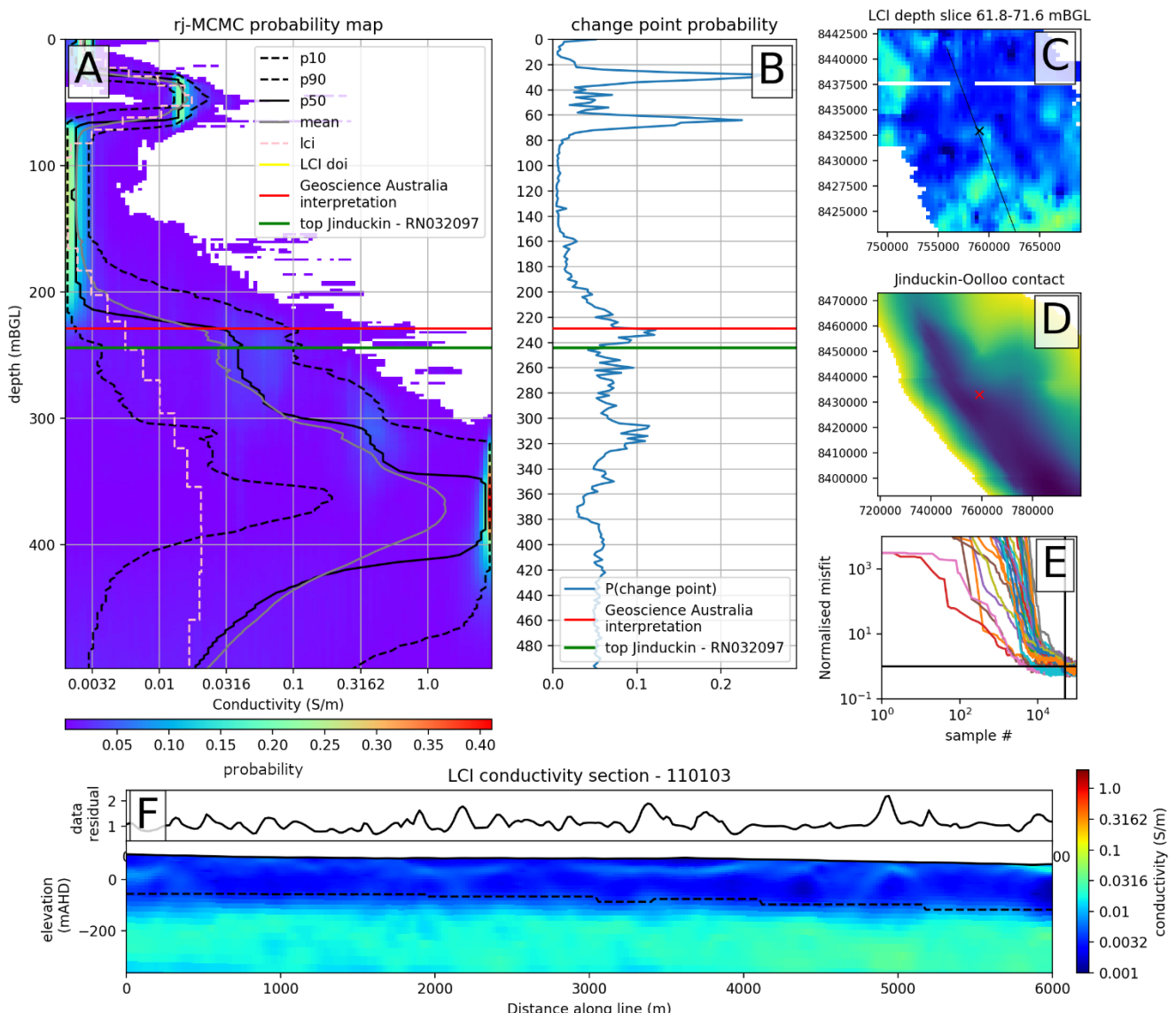


Figure 3.2 The probability map plot for the nearest airborne electromagnetic (AEM) sounding to borehole RN032097, the only stratigraphic hole that is both cored across the Oolloo–Jinduckin boundary and within 500 m of an AEM sounding. The conductivity probability map (panel A) shows that conductivity increases from around 210 mBGL. Our interpreted depth of the interface (229 mBGL) is 15 m shallower than the borehole interpretation of 244 m (Kruse et al., 1990). However, the considerable range between the 10th percentile (p10) and 90th percentile (p90) models indicates considerable uncertainty at these depths. We consider these two interpretations as being consistent given the uncertainty. See Figure 2.2 for a full description of each panel.

Table 3.1 Comparison between the elevation (m AHD) of the Oolloo–Jinduckin interface interpreted from borehole data and the nearest AEM sounding.

Borehole	Borehole easting	Borehole northing	Borehole longitude	Borehole latitude	Borehole elevation (m AHD)	AEM interpreted interface (m AHD)	Borehole interpreted interface (m AHD)	Borehole–AEM xy-distance (m)	(AEM–borehole) Oolloo–Jinduckin elevation z-distance (m)
RN006825	742730.2	8455761	131.24677	-13.95808	61	-140	-138	172	-2
RN032097	758830.1	8432861	131.39786	-14.16354	92	-137	-152	249	15

RN030948	741068.2	8460173	131.23102	-13.91836	40	-127	-96	405	-31
RN031100	740970.2	8460210	131.23011	-13.91804	40	-125	-51	372	-74
RN034340	743653	8462759	131.25470	-13.89478	52	-32	-9	164	-23
RN034303	743904	8463070	131.25699	-13.89195	54	-13	18	494	-31
RN031103	816129.9	8401162	131.93197	-14.44389	159	-9	31	470	-40
RN034304	743252	8463009	131.25097	-13.89255	46	-6	19	417	-25
RN033720	737029	8468948	131.19291	-13.83942	45	-4	-7	373	3
RN021152	739130.1	8467661	131.21245	-13.85087	47	5	17	83	-12
RN033723	737298	8469150	131.19538	-13.83757	45	18	11	435	7
RN020613	736630.2	8469261	131.18919	-13.83662	42	23	17	422	6
RN033369	740319	8467906	131.22342	-13.84856	66	43	30	313	13
RN033010	761743.1	8446468	131.42354	-14.04035	110	44	83	219	-39
RN025288	756986	8449800	131.37921	-14.01068	121	58	53	103	5

3.2 Modelling stratigraphy

We interpreted the depth below ground level of the Oolloo–Jinduckin interface for AEM soundings at 389 locations (Figure 3.3 A). The top of the deeper, more conductive Jinduckin Formation is generally well resolved in the AEM conductivity models throughout most of the modelling area. However, the ability of the AEM to resolve the upper surface and accordingly the certainty of our interpretations decreases with depth. There are no boreholes with co-located AEM soundings in these parts of the basin to constrain our interpretation and we consider the model highly uncertain in areas where depths to the Oolloo–Jinduckin interface exceed about 300 m.

We converted modelled depths to elevation using the digital elevation model from the AEM system. These interface elevations were interpolated to produce the surface detailed in Figure 3.3 A. The interpreted surface reveals a northwest-trending synform, consistent with current understanding of basin architecture. The surface shows considerably steeper dips (up to 6°s) in the southwest and northeast, which could be the result of faulted basin margins (Kruse & Munson, 2013). This surface has a minimum elevation at about -348 m AHD towards the centre of the basin and rises to above 100 m AHD towards the margins of the Oolloo Dolostone.

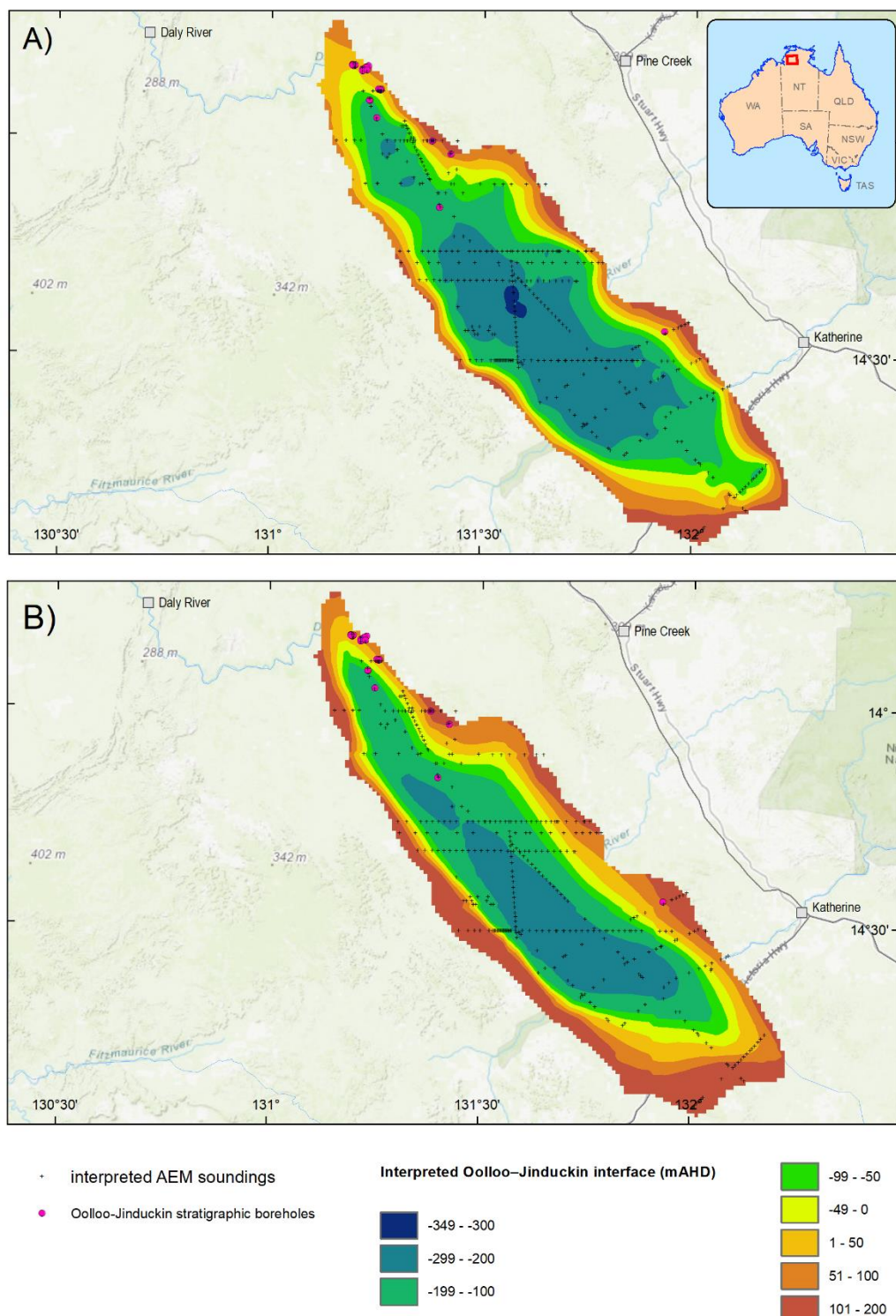


Figure 3.3. A) Newly interpreted Oolloo–Jinduckin interface surface in the Daly Basin. This map also shows the interpreted airborne electromagnetic (AEM) sounding locations and boreholes from the Northern Territory Department of Environment and Natural Resources Water Resources registered bore database that are within 500 m of AEM lines and have an interpreted depth to Oolloo–Jinduckin interface. B) The DENR2018 model interpolated onto the same grid as the GA model in A). Both grids were interpolated using the Topo to Raster algorithm in ArcGIS.

3.3 Comparison with existing Oolloo–Jinduckin surface in DENR2018 model

The new AEM interpretation of the Oolloo–Jinduckin interface was developed with little input from previous interpretations (discussed in Section 4.14.1). To enable a visual comparison, the two surfaces were modelled onto the same grid and are visualised using identical colour stretches in Figure 3.3. The DENR2018 surface (Figure 3.3 B) is smoother than our model, which reflects the small number of stratigraphic bores and the inclusion of hand-drawn contours as a constraint during gridding. In contrast our model is constrained by more data, but includes gridding artefacts due to the uneven distribution of interpreted soundings.

The most obvious difference between the two models is that our model tends to have steeper basin margins. This is most pronounced along the southwest margin, where the GA surface is considerably deeper than the DENR2018 surface. Such differences is not surprising given the scarcity of borehole information. The conductivity section in Figure 3.4 illustrates that the DENR2018 interpretation approaches the shallow surface ~12 km to the east of the AEM interpreted Oolloo–Jinduckin surface, which may explain such significant offsets. Further drill hole or outcrop data are required to test which model most accurate represents this margin.

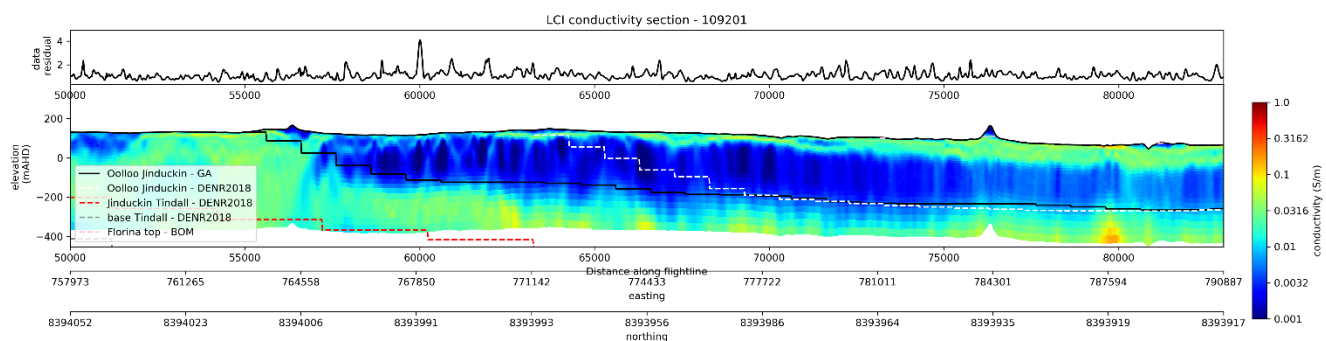


Figure 3.4 Vertically gridded LCI conductivity section of flight line #109201, clipped to the southwest margin of our Oolloo–Jinduckin interface. This section shows that the DENR2018 interpretation intersects the ground surface at ~63,000 m (distance from easternmost point along the flight line) compared to ~55,000 m for the GA interpreted Oolloo–Jinduckin surface (this study). There is no borehole or outcrop data to validate which model is more accurate in this area.

4 Discussion

4.1 Methodology appraisal and new interpretation

As we discussed in Section 2.3, interpreting stratigraphy from AEM conductivity models is not simple. As stratigraphic units have distinct properties, we may expect them to also have characteristic bulk conductivities. This is often true for clastic sedimentary aquifers where there may be a strong positive correlation between bulk conductivity and fraction of clay (e.g. Foged et al., 2014). However, this may not always be the case, particularly in areas with variable groundwater quality, saturation, porosity and/or cementation. An interpreter must, at the outset, ascertain that the stratigraphic units have distinct bulk conductivities before attempting to model boundaries of these units using AEM.

The AEM conductivity models on which we make our stratigraphic interpretations are always uncertain. Sources of model uncertainty include measurement error, simplifying assumptions about the relationship between sub-surface properties and geophysical observation, poor data fits and model non-uniqueness. An interpreter should also ascertain that the stratigraphic boundary is resolvable with AEM data given these uncertainties (Ray et al., 2020a). Thus, we should approach stratigraphic interpretation with a good handle on not only AEM model uncertainty but also the geophysical properties of the units that are being modelled.

In this study, we examine a stratigraphic interface that can be interpreted from AEM models with relatively high confidence. Throughout the mapped extent of the Oolloo Dolostone in the Daly Basin, we observe a resistive body above a more conductive body (i.e. Jinduckin Formation) at depths up to 400 m below surface (see Figure 2.2, Figure 2.3, Figure 3.1 and Figure 3.4). The boundary between these two units forms a gently dipping synform with a geometry broadly consistent with previous models of basin architecture. Fortunately, there does not appear to be widespread variation in groundwater salinity or other variables that could obscure this interface. We have demonstrated that this boundary approximately corresponds to the interpreted transition between the Jinduckin Formation and overlying Oolloo Dolostone by systematically comparing our picks to interpretations from nearby stratigraphic boreholes.

AEM is inherently well suited to modelling this stratigraphic boundary, as it is most sensitive to measuring conductivity in the top few hundred metres of the sub-surface (Ley-Cooper, 2016; Ray et al., 2020a). Further, AEM is better at resolving the top of conductive units than the bottom due to conductivity thickness trade-offs and the more rapid attenuation of the AEM signal if there is overlying conducting material (Blatter et al., 2018). We have attempted to arm the interpreter with an understanding of model uncertainty by interpreting directly from the posterior distribution of conductivity (Figure 2.2 and Figure 2.3). The probability map visualisations, developed as part of this study, are information-rich and reduce the need for the interpreter to navigate different displays, thus reducing cognitive effort and increasing efficiency.

One approach to ‘evaluating’ our modelled interface is to compare our interpretation with interpretations derived independently of the AEM. In Section 3.1 we demonstrated that borehole stratigraphic interpretations do not always agree with our interpretation (Root Mean Square (RMS) difference = 28.5 m). While such disagreement may be concerning on face value, we do not consider that there is enough certainty in the borehole interpretations to invalidate our model even at locations with high offsets.

A major reason for the lower confidence in borehole interpretation is that the only cored boreholes that intersect the Oolloo–Jinduckin interface are NTGS86/1 (RN032097) and KRVH1 (Kruse et al., 1990; Tickell, 2011, Figure 2.1). Hence the criteria for picking the Oolloo–Jinduckin from borehole data was developed using observed relationships from two bores. Of these, only NTS86/1 had a nearby AEM sounding which we could use to visualise the relationship between stratigraphy and bulk conductivity (see Section 3.1 and Figure 3.2).

At the boreholes summarised in Table 3.1 the Oolloo–Jinduckin interface was interpreted using gamma logs or driller's logs. Where the interpretation differences were considered excessive given AEM interpretation uncertainties, we examined the borehole data. In almost all cases the borehole stratigraphic interpretations were not certain enough to reject the AEM interpretation. Hence, we conclude that, while the AEM data and borehole interpretations do not always agree, the AEM-based interpretation was not at all inconsistent with the borehole data.

At this point, it is worth questioning if offsets between interpretations may be because the borehole and the AEM interpretations are not picking the same physical horizon. The top of the Jinduckin Formation from the borehole is interpreted using the 'highest finely laminated dolomitic sandstone–siltstone interbeds' (Tickell, 2011), whereas in the AEM data we generally picked the point below which there is an appreciable increase in conductivity (Section 2.4). We might expect that the larger clay fraction within these laminated siltstone interbeds may be the driver of increased conductivity and that these criteria should yield similar depth estimates. However, this may not always be the case, especially as the boundary is conformable and gradational. More co-located conductivity and gamma data are needed across this interval to further explore this possibility.

Thus far we have discussed model accuracy in areas with borehole control. In areas with very little other information, we are unable to independently evaluate the performance of the new interpretation against other datasets. Thus, for most of the basin, we can only conclude that the Oolloo–Jinduckin surface is both consistent with our best understanding of the AEM data and geologically reasonable given our understanding of the basin architecture. However, this surface is almost certainly overly smoothed as we made no attempt to explicitly include basin faults during either the interpretation or the interpolation. New drilling information from data-sparse areas would allow us to further refine our model and test our current assumptions, especially where the interface is deeper in the sub-surface.

From the discussion above we conclude that the AEM is suitable for the interpretation of the Oolloo–Jinduckin interface. The interface appears well resolved in the conductivity models and the interpreter had easy access to a range of interactive interpretation products showing both deterministic and stochastic models. However, an evaluation of the accuracy of the modelling is difficult, as the stratigraphic interpretations from bores are problematic. Our modelled interface is consistent with our present understanding of the Daly Basin and we believe this is a strong contribution to our understanding of basin architecture.

4.2 Hydrogeological implications

The hydrogeological implications of our interpretation of the Oolloo–Jinduckin are important. If we were to accept our model as being superior to the DENR2018 model in data sparse areas, then we might expect a significant increase in the volume of the Oolloo aquifer, particularly around the margins. The new interface could be used to refine groundwater flow or coupled surface water – groundwater model in the Daly Basin. This may inform ongoing management of water resources and help to refine models of sustainable yields from the Oolloo aquifer.

Another potential benefit of our modelled interface is in defining the deeper stratigraphic contact between the Jinduckin Formation and the Tindall Limestone. Currently, this interface is very poorly constrained, especially in the centre of the basin, where there is virtually no deep drilling information. The Daly Group is thought to have formed through continued sedimentary deposition with mild sagging. In this scenario we expect the Jinduckin–Tindall interface to have a linear relationship to the shallower, better constrained Oolloo–Jinduckin interface. Thus, the newly modelled interface in this study could inform the modelling of the deeper interface in areas with little borehole control. Further work would be required to explore if differential movement on basin margin faults during the evolution of the basin could undermine this relationship. Once again, a more realistic estimate of the depth to the surface of the Tindall Limestone aquifer can be used as an input to groundwater flow models, which may improve management of water resources from this aquifer.

5 Conclusions

In this study we have used both deterministic and stochastic inversions of the Daly Basin AEM data to interpret the subsurface depths of the Oolloo–Jinduckin interface and map its extent. Despite the economic, environmental and cultural importance of the Oolloo Dolostone aquifer, the interface with the underlying aquitard is poorly constrained in many areas. The siltstone rich, Jinduckin Formation is significantly more electrically conductive than the overlying Oolloo Dolostone and the stratigraphic transition can be resolved in the AEM conductivity model throughout the basin. The interface can be modelled with reasonable confidence in all areas except the deeper parts (>300 m depth) of the basin. However, a lack of high-quality borehole data within the basin limits our ability to independently validate the interpretation. Our AEM-derived Oolloo–Jinduckin interface suggests that the DENR2018 model generally underestimates the depth of the base of the Oolloo Dolostone Aquifer, especially in areas where other subsurface data are sparse. In particular, the lack of borehole data in the southwest margin has resulted in significant differences. The newly interpreted surface is geologically consistent with models of basin formation and provides a basis for review of the current groundwater flow modelling.

As part of this investigation, we developed a new method for stratigraphic interpretation using deterministic and stochastic AEM inversion products. This approach demonstrates that the inevitable uncertainty resulting from geophysical inversion can be incorporated into the interpretation process. This approach has potential for use future projects that involve interpreting stratigraphy from stochastic geophysical inversions.

6 Recommendations

This work enhances our understanding of the stratigraphy and structure of the Daly Basin, although the newly defined Oolloo–Jinduckin interface is not particularly well validated by other field data. To improve the modelled interface, we suggest a more detailed investigation including integration of all available hydrogeological and geophysical data. The validity of our findings would particularly benefit from high-quality drill holes that intersect the Oolloo–Jinduckin interface near AEM soundings, particularly in areas where our model significantly disagrees with the DENR2018 model. Additional induction and gamma log data from across this stratigraphic boundary would also be beneficial, as it would give us a much greater handle on the relationship between lithology and conductivity in the basin.

In this study we used stochastic AEM inversions to understand the uncertainty of our interpretations. Our methodology could be improved by adding uncertainty estimates to our interpretations using the change point probability histogram (Figure 2.2b). This approach could allow geological uncertainty to be better quantified and propagated into future modelling endeavours.

Our Oolloo–Jinduckin surface dips up to 6° on the northeast and southwest margins and near the centre of the basin. If these steeper dips are the manifestation of basin scale faults, it may have implications for geological modelling of the Tindall Limestone. Drilling, seismic imaging or potential field methods may be suited for this investigation.

Acknowledgements

Geoscience Australia's groundwater expertise is based on strong collaboration with state and territory governments, academia, landholders and traditional owners. For this project we would especially like to thank the Northern Territory Department of Environment and Natural Resources for collaborating on this project with us. This report was greatly improved by reviews from Tim Evans, Steve Lewis and Merrie-Ellen Gunning. We would like to thank the Ross C. Brodie, Yusen Ley-Cooper and Richard Taylor for work on the GARJCMCDEM algorithm and ideas for visualising the outputs.

References

- Auken, E., Christiansen, A.V., Jacobsen, B.H., Foged, N. & Sørensen, K.I. 2005. Piecewise 1D laterally constrained inversion of resistivity data. *Geophysical Prospecting*, 53(4), 497-506.
- Blatter, D., Key, K., Ray, A., Foley, N., Tulaczyk, S. & Auken, E. 2018. Trans-dimensional Bayesian inversion of airborne transient EM data from Taylor Glacier, Antarctica. *Geophysical Journal International*, 214(3), 1919-1936.
- Bureau of Meteorology. 2017. AUSTRALIAN GROUNDWATER EXPLORER 3D Aquifer Visualisation—Cambrian Limestone Aquifers, NT.
http://www.bom.gov.au/water/groundwater/explorer/pdf/3d_daly_NT.pdf
- Brodie, R.C. & Richardson, M. 2015. Open source software for 1D airborne electromagnetic inversion. *ASEG Extended Abstracts*, 2015(1), 1-3.
- CSIRO. 2009. Water in the Daly region of the Timor Sea Drainage Division. *A report to the Australian Government from the CSIRO Northern Australia Sustainable Yields Project*. CSIRO Water for a Healthy Country Flagship Australia, xl.
- Foged, N., Marker, P.A., Christansen, A.V., Bauer-Gottwein, P., Jørgensen, F., Høyer, A.-S. & Auken, E. 2014. Large-scale 3-D modeling by integration of resistivity models and borehole data through inversion. *Hydrology and Earth System Sciences*, 18(11), 4349-4362.
- Hutchinson, M.F. 1989. A new procedure for gridding elevation and stream line data with automatic removal of spurious pits. *Journal of Hydrology*, 106(3), 211-232.
- Kirkegaard, C., Sonnenborg, T.O., Auken, E. & Jørgensen, F. 2011. Salinity distribution in heterogeneous coastal aquifers mapped by airborne electromagnetics. *Vadose Zone Journal*, 10(1), 125-135.
- Kluyver, T., Ragan-Kelley, B., Pérez, F., Granger, B.E., Bussonnier, M., Frederic, J., Kelley, K., Hamrick, J.B., Grout, J., Corlay, S., Ivanov, P., Avila, D., Abdalla, S., Willing, C. & Jupyter development team. 2016. Jupyter notebooks—a publishing format for reproducible computational workflows. Loizides, Fernando and Scmidt, Birgit (eds.) In *Positioning and Power in Academic Publishing: Players, Agents and Agendas*. IOS Press. pp. 87-90.
- Knapton, A. 2005. *Preliminary groundwater modelling of the Ooloo Dolostone: a report prepared by NRETA*. Northern Territory Government.
<http://www.territorystories.nt.gov.au/jspui/handle/10070/251010>
- Knapton, A. 2006. *Regional groundwater modelling of the Cambrian limestone aquifer system of the Wiso, Georgina and Daly Basins*. Northern Territory Government.
<http://www.territorystories.nt.gov.au/jspui/handle/10070/228069>
- Knapton, A. 2011. *Technical report—National Water Commission low flows project: case study—recalibration of a coupled surface water – groundwater model to the low flows in the Daly River Catchment*. Northern Territory Government.
<http://www.territorystories.nt.gov.au/jspui/handle/10070/252705>

Knapton, A., Jolly, P., Harrington, G., Pethram, C., Water, C.L. & DENR. 2010. *Northern Australia sustainable yields project: an investigation into the effects of climate change and groundwater development scenarios on the water resources of the Daly River Catchment using an integrated groundwater/surface water model*. Northern Territory Government.

<http://www.territorystories.nt.gov.au/jspui/handle/10070/252782>

Korus, J.T., Joeckel, R.M., Divine, D.P. & Abraham, J.D. 2017. Three-dimensional architecture and hydrostratigraphy of cross-cutting buried valleys using airborne electromagnetics, glaciated Central Lowlands, Nebraska, USA. *Sedimentology*, 64(2), 553-581.

Kruse, P.D., Whitehead, B.R. & Mulder, C.A. 1990. *Tipperary, Northern Territory: explanatory notes*. Northern Territory Geological Survey. Viewed 15 April 2020.
<https://geoscience.nt.gov.au/gemis/ntgsjpsui/handle/1/81893>

Kruse, P.D. & Munson, T.J. 2013. Daly Basin. In: Ahmad M. & Munson T.J. (compilers). *Geology and mineral resources of the Northern Territory*. Special Publication 5, chap. 31. Northern Territory Geological Survey, Darwin.

Ley-Cooper, A.Y. 2016. Dealing with uncertainty in AEM models (and learning to live with it). *ASEG Extended Abstracts*, 2016(1), 1-6.

Ray, A., Symington, N., Ley-Cooper, Y. & Brodie, R.C. 2020a. *A quantitative Bayesian approach for selecting a deterministic inversion model*. Exploring for the Future: Extended Abstracts. Geoscience Australia, Canberra.

Ray, A., Cathro, D., Hostetler, S., Symington, N., Carey, H. & Peljo, M. 2020b. *Daly River Region AEM SkyTEM airborne electromagnetic survey*. Geoscience Australia, Canberra.,
<http://pid.geoscience.gov.au/dataset/ga/122012>

Roach, I. & McPherson, A. 2016. *Cover characterisation and shallow basement mapping using airborne electromagnetic data: examples from the Southern Thomson Project*.

Siemon, B., Christiansen, A.V. & Auken, E. 2009. A review of helicopter-borne electromagnetic methods for groundwater exploration. *Near Surface Geophysics*, 7(5-6), 629-646.

Symington, N., Ray, A., Harris-Pascal, C., Tan, K., Ley-Cooper, Y. & Brodie, R. 2020. *Salinity classification using borehole and AEM data: a framework for uncertainty analysis*. Exploring for the Future: Extended Abstracts. Geoscience Australia, Canberra.

Tarantola, A. 2006. Popper, Bayes and the inverse problem. *Nature Physics*, 2(8), 492-494.

Tickell, S. 2011. *Subsurface characteristics of the Oolloo Dolostone*. Technical Report 28/2011. Northern Territory Government. <http://www.territorystories.nt.gov.au/jspui/handle/10070/238413>

Tickell, S.J., Kruse, P.D. & Munson, T.J. 2015. Daly Basin, Northern Territory: lithostratigraphic revision resolves context of incongruous Ordovician fossils. *Australian Journal of Earth Sciences*, 62(6), 743-760.

Tickell, S.J. 2009. *Groundwater in the Daly Basin*. Technical Report No. 27/2008D. Northern Territory Department of Natural Resources, Environment, the Arts and Sport.

Viezzoli, A., Munday, T. & Ley-Cooper, Y. 1997. Airborne electromagnetics for groundwater salinity mapping: Case studies of coastal and inland salinisation from around the world. *Bollettino Di Geofisica Teorica Ed Applicata*, 7(4), R126.